Stanford Exploration Project, Report 73, November 18, 1997, pages 311–320

Stanford Exploration Project, Report 73, November 18, 1997, pages 311–320

Short Note

Time-to-depth conversion

Lin Zhang[1]

keywords: *ray tracing, diffraction, imaging, velocity*

INTRODUCTION

It is well known that, even if correct velocity information is provided, any conventional time-migration algorithm outputs erroneous images of subsurface structures whenever overburden velocities vary laterally. Depth migration has been demonstrated to be superior to time migration in handling general velocity variations. However, even today, time migration is still widely used in industry. Black and Brzostowski (1992) gave two reasons to explain the continued wide-spread use of time migration. Their first reason concerns computational costs. They estimated that depth migration usually requires an order of magnitude more computer time than time migration. With today's computer power, such a cost ratio can become significant when data collected in a moderate-sized 3-D survey are to be imaged. The second reason is related to the sensitivity of a migration process to velocity errors. Numerical experiments show that time migration is less sensitive to velocity errors than depth migration and is thus useful in starting an iterative algorithm of migration-velocity analysis. I believe that another reason that may extend the use of time migration in the future is the possibility of developing efficient algorithms with which a time-migrated image can be converted into the corresponding depth-migrated image. In this paper, I refer to this type of algorithms as time-to-depth conversion.

The simplest algorithm for time-to-depth conversion is to stretch the vertical axis of a time-migrated image in accordance with the relation between the vertical traveltime and depth. Obviously, such an algorithm is valid only for layered media. Assuming that time migration focuses the energy diffracted from a scatterer to a point, Hubral (1977) introduced the concept of the image ray that defines a time-to-depth conversion valid for arbitrary variations of overburden velocities. The cascade of time migration and image-ray corrections was later proposed (Larner et. al., 1981) as an approximation to true depth migration. Experiments with field data show that the image-ray corrections are often important in the presence of lateral velocity variations. Black and Brzostowski (1992) recently studied the errors of time migration

[1]**email:** not available

and pointed out that the image-ray method is invalid for reflectors of large dips. They suggested that image-ray corrections should be supplemented by additional spatial corrections.

One of the most important applications of the image ray method is in the process of migration-velocity analysis that usually requires an efficient prestack migration algorithm. However, up till now, the concept of image ray is limited to poststack imaging and the computation of image rays is done through ray tracing that is inefficient. In this paper, I present my studies in two aspects of the image-ray method. Assuming that the validity condition of the image ray method holds, I generalize the image-ray concept to prestack imaging. I derive the mapping functions of the image-ray corrections for both profile imaging and constant offset imaging. I also describe how to compute these mapping functions without actually tracing image rays. For the sake of simplicity, I address the problem only in two-dimensional cases although the concepts and algorithms readily generalize to three dimensions.

REVIEW OF HUBRAL'S IMAGE-RAY CONCEPT

Before describing the image-ray method for prestack imaging, let me first review Hubral's image-ray concept for poststack imaging. On a stacked section, the energy diffracted from a point scatterer is distributed among signals upon its traveltime curve referred to as the diffraction curve. Although the diffraction curve becomes non-hyperbolic when overburden velocities of the scatterer vary laterally, it usually is well approximated by a hyperbola in the vicinity of its apex. Hence, the energy distributed over this portion of the curve can be focused around the apex position by time migration. To determine the depth-migrated position of the focused energy, Hubral (1977) introduced the concept of the image ray. According to his definition, image rays are the propagation paths of the energy in the signals at the apex positions of diffraction curves. Because diffraction curves have zero time-slope at their apex positions, all image rays shoot vertically at the surface. Suppose that an image ray connects surface point x_0 and subsurface point (x, z), and that the two-way traveltime along this ray is t_0. Then, the energy diffracted from a point scatterer at (x, z) is distributed along the diffraction curve whose apex is at (t_0, x_0). Consequently, if we assume that time migration focuses the energy along the diffraction curve onto the apex position of the curve, the mapping from (t_0, x_0) to (x, z) defines a general time-to-depth conversion for poststack imaging.

Let us suppose that we have a stacked section $P(t, x_r)$. If we depth-migrate this section, we would get the correct image $Q(x, z)$. However, if we use a conventional time-migration to image this section, we obtain a time-migrated image $P_0(t_0, x_0)$. By tracing the image ray for each subsurface point (x, z), we can find two mapping functions of the time-to-depth conversion, as follow:

$$\begin{cases} t_0 = 2\tau_0(x,z) \\ x_0 = \lambda_0(x,z), \end{cases} \tag{1}$$

where $\tau_0(x,z)$ and $\lambda_0(x,z)$ are the one-way traveltime and surface location of the image ray that reaches the subsurface point (x,z), respectively. As the result, the time-to-depth conversion becomes a variable-substitution process, as follows:

$$Q(x,z) = P_0(2\tau_0(x,z), \lambda_0(x,z)). \tag{2}$$

Apart from amplitude considerations, this conversion correctly positions the focused images of subsurface structures.

GENERALIZED IMAGE-RAY METHOD

The image ray method for poststack imaging assumes that time migration focuses the energy diffracted from a scatterer onto the apex of the diffraction curve. All what the image-ray corrections do is to map the image sample at the time-migrated position of the apex to the depth-migrated position of the scatterer. In this section, I use the same assumption and concept to generalize the image-ray method to prestack imaging.

Profile imaging

Let us first study the generalized image-ray method for profile imaging. Figure **??** shows the ray paths in a common shot experiment. The seismic energy generated by a shot at surface location x_s propagates towards a point scatterer at subsurface position (x,z). After being diffracted from the scatterer, the energy travels along the multiple ray paths connecting the scatterer to each receiver of a receiver array. On the recorded shot gather, the seismic energy is distributed in the data samples along a diffraction curve that is determined by the functional relationship between traveltime t and receiver location x_r. The diffraction curve has a hyperbolic shape when the overburden velocities of the scatterer are free of lateral variations. If we assume that the lateral velocity variations are confined to a reasonable scale, this curve usually is well fit by a hyperbola in the vicinity of its apex. Consequently, a profile time-migration can collapse the energy distributed over this portion of the diffraction curve.

If time migration is implemented by using a Kirchhoff summation, the time-image sample at (t_0, x_0) is the weighted sum of data samples along a migration curve, as follows:

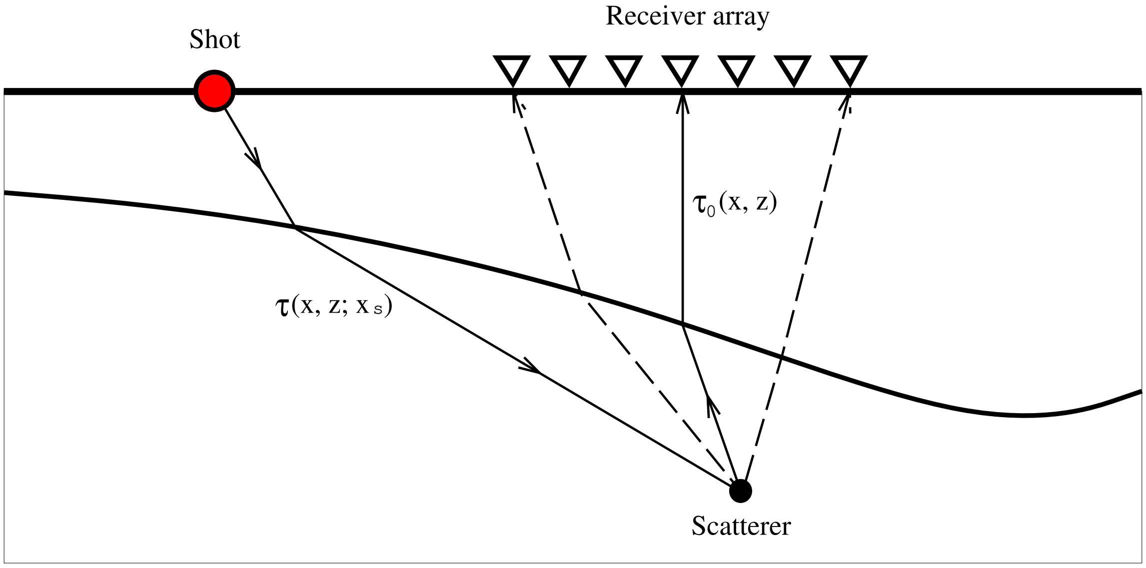

Figure 1: Ray paths in a common shot experiment. The solid line shows an image ray. lin2-imraycsg [NR]

$$t = \sqrt{t_0^2 + \frac{(x_s - x_0)^2}{v_m^2}} + \sqrt{t_0^2 + \frac{(x_r - x_0)^2}{v_m^2}}, \tag{3}$$

where v_m is a migration velocity. For a given shot location x_s, this equation defines traveltime t as a function of receiver location x_r. By taking the derivative of traveltime t in equation (3) with respect to receiver location x_r and setting the result to zero, we can find the coordinates of the apex of the migration curve for given (t_0, x_0), as follows:

$$\left\{ \begin{array}{lcl} t_a & = & \sqrt{t_0^2 + \frac{(x_s - x_0)^2}{v_m^2}} + t_0 \\ \\ x_a & = & x_0. \end{array} \right. \tag{4}$$

Thus, the Kirchhoff time-migration focuses the diffracted energy along the diffraction curve whose apex is at (t_a, x_a) to the point (t_0, x_0) of the time-migrated image. The correct time-to-depth conversion should map the image sample at (t_0, x_0) to the true position (x, z) of the scatterer.

To find the apex position of the diffraction curve, I define image rays for profile imaging to be the propagation paths of the energy in the signals at the apex positions of diffraction curves on a common shot gather. At the apex of a diffraction curve, the derivative of the traveltime with respective to the receiver location is zero. Therefore, an image ray emerges vertically at the receiver location. Figure **??** shows an example of such an image ray. By tracing the image ray passing through the scatterer at subsurface position (x, z), we can find the coordinates of the apex position of the diffraction curve, as follows:

$$\begin{cases} t_a = \tau(x, z; x_s) + \tau_0(x, z) \\ \\ x_a = \lambda_0(x, z), \end{cases} \tag{5}$$

where $\tau(x, z; x_s)$ is the traveltime from shot location x_s to subsurface position (x, z), and $\tau_0(x, z)$ and $\lambda_0(x, z)$ are the same as defined in equation (1). Combining equations (5) and (3) gives us the mapping functions of the time-to-depth conversion, as follows:

$$\begin{cases} t_0 = \dfrac{[\tau(x, z; x_s) + \tau_0(x, z)]^2 - \dfrac{(x_s - \lambda_0(x, z))^2}{v_m^2}}{2[\tau(x, z; x_s) + \tau_0(x, z)]} \\ \\ x_0 = \lambda_0(x, z) \end{cases} \tag{6}$$

Once these two mapping functions are computed, the image-ray corrections for profile imaging is again a variable-substitution process.

Constant offset imaging

Because a constant offset section is an offset continuation of a zero offset section, I assume that the diffraction curve on a constant offset section is well approximated by a flat top hyperbola in the vicinity of its apex when the lateral velocity variations are confined to a reasonable scale. Consequently, a constant offset time-migration can collapse the energy distributed over this portion of the diffraction curve.

For a given time image position (t_0, x_0), the migration curve of the constant-offset Kirchhoff summation is:

$$t = \sqrt{t_0^2 + \frac{(m - h - x_0)^2}{v_m^2}} + \sqrt{t_0^2 + \frac{(m + h - x_0)^2}{v_m^2}}, \tag{7}$$

where v_m is a migration velocity, m and h are midpoint and half offset, respectively. For a given half offset h, this equation defines traveltime t as a function of midpoint m. The coordinates of the apex of the migration curve are:

$$\begin{cases} t_a = 2\sqrt{t_0^2 + \dfrac{h^2}{v_m^2}} \\ \\ m_a = x_0. \end{cases} \tag{8}$$

Thus, the Kirchhoff time-migration focuses the diffracted energy along the diffraction curve whose apex is at (t_a, m_a) to the point (t_0, x_0) of the time-migrated image. The correct time-to-depth conversion should map the image sample at (t_0, x_0) to the true position (x, z) of the scatterer.

Similarly to profile imaging, I define image rays for constant offset imaging to be the propagation paths of the energy in the signals at the apex positions of diffraction curves on a constant offset section. At the apex of the diffraction curve, the derivative of the traveltime with respective to the midpoint location is zero. We know that the traveltime is $\tau(x, z; m-h) + \tau(x, z; m+h)$. If we define $p(x, z; x_s)$ to be the partial derivative of $\tau(x, z; x_s)$ with respect to x_s, then image rays for constant offset imaging satisfy the following relation:

$$p(x, z; m-h) + p(x, z; m+h) = 0. \tag{9}$$

Figure **??** shows an example of such an image ray. By tracing the image ray passing through the scatterer at subsurface position (x, z), we can find the coordinates of the apex position of the diffraction curve, as follows:

$$\left\{ \begin{array}{lcl} t_a & = & \tau(x, z; m-h) + \tau(x, z; m+h) \\ \\ m_a & = & \{m \mid p(x, z; m-h) + p(x, z; m+h) = 0\}. \end{array} \right. \tag{10}$$

Combining equations (10) and (7) gives us the mapping functions of time-to-depth conversion, as follows:

$$\left\{ \begin{array}{l} t_0 = \sqrt{\frac{1}{4}[\tau(x, z; m-h) + \tau(x, z; m+h)]^2 - \frac{h^2}{v_m^2}} \\ \\ x_0 = \{m \mid p(x, z; m-h) + p(x, z; m+h) = 0\}. \end{array} \right. \tag{11}$$

Because these two mapping functions contain an implicit function, the image-ray corrections for constant offset imaging is more difficult than one for profile imaging.

EFFICIENT COMPUTATIONS OF IMAGE RAYS

The mapping functions for the time-to-depth conversion are previously computed by tracing image rays. The method gives the mapping functions along the image rays. Mapping time-migrated image along the image rays subsequently gives the depth-migrated image that has to be interpolated onto a regular grid. For complicated velocity models, image ray may cross each other or not penetrate shadow zones; the interpolation is thus cumbersome and computationally expensive. In this section, I describe an efficient algorithm for computing the mapping functions of the image-ray corrections on a regular grid,

To compute the functions $\tau_0(x, z)$ and $\lambda_0(x, z)$ in equation (1), we consider two partial differential equations. Because all image rays shoot vertically when leaving

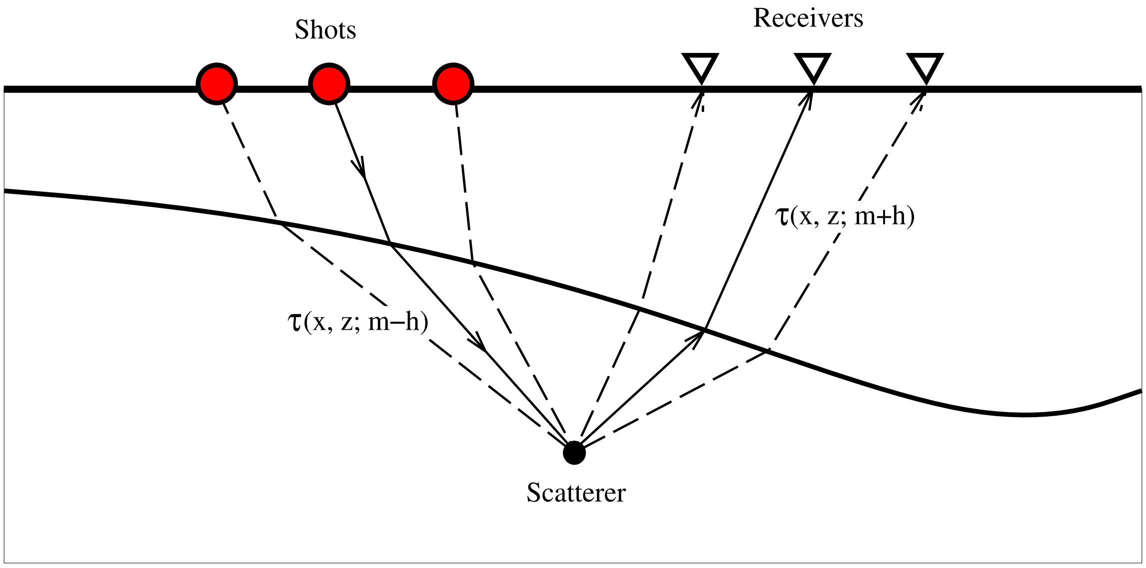

Figure 2: Ray paths in a constant offset experiment. The solid line shows an image ray. lin2-imraycos [NR]

the surface, they are associated with a vertically incident plane wavefront. The value of function $\tau_0(x, z)$ is the traveltime for the wavefront to propagate from the surface to a subsurface point (x, z), which satisfies the eikonal equation:

$$\left(\frac{\partial \tau_0}{\partial x}\right)^2 + \left(\frac{\partial \tau_0}{\partial z}\right)^2 = \frac{1}{v^2(x, z)}, \tag{12}$$

with the initial condition $\tau_0(x, 0) = 0$. The value of function $\lambda_0(x, z)$ is the initial surface position of the image ray that eventually reaches a subsurface point (x, z). This function is thus constant along each image ray. Using the orthogonal relation between rays wavefronts in a isotropic medium, we can show that this function satisfies the partial differential equation as follow:

$$\left(\frac{\partial \tau_0}{\partial x}\right)\left(\frac{\partial \lambda_0}{\partial x}\right) + \left(\frac{\partial \tau_0}{\partial z}\right)\left(\frac{\partial \lambda_0}{\partial z}\right) = 0, \tag{13}$$

with the initial condition $\lambda_0(x, 0) = x$.

Two partial differential equations (12) and (13) can be solved simultaneously by using an up-wind finite difference method (Zhang, 1991), and the results are samples of the two mapping functions on a regular grid. Thus, the image-ray corrections can be implemented with an algorithm summerized, as follow:

```
for each x_j
[
    for each z_i
    [
        t̂_0 = τ_0(z_i, x_j)
        x̂_0 = λ_0(z_i, x_j)
        Q(z_i, x_j) = Interpolation of P_0(t_0, x_0)  onto  (t̂_0, x̂_0)
```

The functions $\tau(x, z; x_s)$ and $p(x, z; x_s)$ in equations (6) and (11) can be computed in a similar way. Two partial differential equations

$$\left(\frac{\partial \tau}{\partial x}\right)^2 + \left(\frac{\partial \tau}{\partial z}\right)^2 = \frac{1}{v^2(x, z)}, \tag{14}$$

and

$$\left(\frac{\partial \tau}{\partial x}\right)\left(\frac{\partial p}{\partial x}\right) + \left(\frac{\partial \tau}{\partial z}\right)\left(\frac{\partial p}{\partial z}\right) = 0, \tag{15}$$

are solved with the point-source initial conditions. The implementation of image-ray corrections for prestack imaging is similar to poststack imaging.

CONCLUSIONS

I have presented an efficient algorithm for image ray corrections and an extension of image ray method to prestack imaging. The theoretical aspects of these new results are quite promising in the application of iterative migration velocity analysis, but their actual effectiveness still subjects to the experiments with synthetic and field data.

ACKNOWLEDGMENTS

I would like to thank Dr. J.L. Black of IBM for many interesting discussions.

REFERENCES

Hubral, P., 1977, Time migration — some ray theoretical aspects: Geophysical Prospecting, **25**, 738-745.

Larner, K.L., Hatton, L., Gibson, B.S., and Hsu, I.G., 1981, Depth migration of imaged time sections: Geophysics, **46**, 734-750.

Black J.L., and Brzostowski M.A., 1992, Systematics of time-migration Errors: Submitted to Geophysics.

Zhang L., 1991, Applying finite-difference method to ray tracing: SEP–**70**, 257-266.